

CAD-based simulations and design of experiments for determining thrust force in drilling operations

Panagiotis Kyratsis^{a,*}, Nikolaos Bilalis^b, Aristomenis Antoniadis^b

^a Technological Educational Institution of West Macedonia, Kila Kozani, GR50100, Greece

^b Technical University of Crete, University Campus, Kounoupidiana, Chania GR73100, Greece

ARTICLE INFO

Article history:

Received 12 February 2011

Accepted 5 June 2011

Keywords:

CAD-based manufacturing

Design of experiments

Regression analysis

Drilling thrust force

ABSTRACT

Drilling thrust force calculations require a large amount of experimental work, which can be greatly reduced, since an extensively validated CAD-based approach, using the DRILL3D software application, has become available. DRILL3D calculates the thrust force of both the cutting areas of the tool (main edges and chisel edge) simultaneously, which means that every simulation can substitute two separate lab experiments. Nevertheless, as the number of parameters involved is increasing, the amount of the necessary simulations becomes substantial. This is the reason that led to the combined use of the DRILL3D and the design of experiments methodology, which reduces the amount of the necessary digital experiments to an impressive degree. The main factors affecting the current analysis are the tool diameter, the web to diameter ratio, the feed rate and the cutting speed used. Using an L16 Taguchi table, a function of the developed thrust force can be calculated using the response surface methodology. This statistical modeling tool employs the regression analysis to establish the relationship between various process parameters and response.

© 2011 Elsevier Ltd. All rights reserved.

1. Introduction

Hole drilling is by far the most widely used process in manufacturing. Although it appears to be a relatively simple process, it is actually a very complex one. One has to consider that, there are two basic tool areas, the main cutting lips and the chisel edge, where thrust force is generated. The drilling point's chisel edge is dominant at the generation of the tool thrust force, while the torque is heavily depended on the action of the cutting lips [1].

Researchers have used a number of different approaches, when simulating drilling, in order to be able to describe accurately the complexity as well as to calculate thrust forces, torques, temperatures, tool wear etc. Three main directions have been adopted over the years.

1. The analytical mathematical approach, where the drilling tool is analytically described by complicated equations in 3D space and used for rigorous geometrical calculations of the drilling process. In a great deal of research efforts, 2D projected geometry is used instead, in order to reduce the amount of calculations necessary [2–6].
2. The experimental one, where an extensive amount of experiments take place and the results are stored in databases so that

different parameters can be used for experimentally derived equations [7–10].

3. The numerical approach, where methodologies such as the finite element analysis are used, based on the Lagrangian and Eulerian methods [11–16].

In an increasing amount of cases, researchers use modern statistical and artificial intelligence tools, in order to reduce the amount of experiments needed and derived equations based on these methods, without performing extensive experiment plans [17–24].

The current paper focuses on the combination of CAD-based drilling simulation and design of experiments. Thrust force calculations require a large amount of experimental work, which can be greatly reduced, since the CAD-based approach has been extensively validated via the DRILL3D software application, built especially for that [25,26]. Nevertheless, as the number of parameters is increasing, so does the magnitude of the necessary experimental work. This is the main reason that led to the combined use of the DRILL3D and the design of experiments methodology, which limits the amount of the necessary digital experiments to an impressive degree.

2. The CAD-based methodology

A modern CAD system, together with its API (Application Programming Interface), can be used to automate a number of

* Corresponding author. Tel.: +30 24610 68294.

E-mail addresses: pkyratsis@hotmail.com, pkyratsis@teikoz.gr (P. Kyratsis), bilalis@dpem.tuc.gr (N. Bilalis), antoniadis@dpem.tuc.gr (A. Antoniadis).

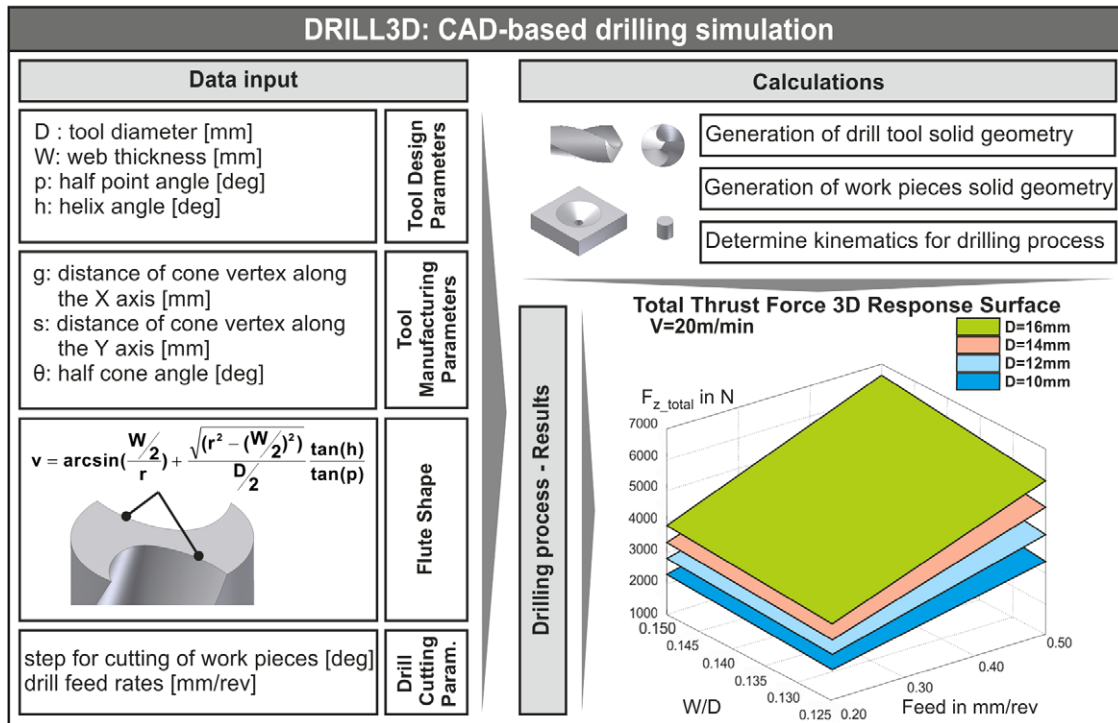


Fig. 1. DRILL3D simulation workflow.

steps toward manufacturing simulations. Different drill tools and work pieces can be created parametrically and an appropriate virtual motion can be programmed, in order to produce all the necessary solid models of the undeformed chips. Using these models, the thrust force of the tool can be calculated for every tool–work-piece material and geometry combination, using a database containing the appropriate experimental coefficients.

DRILL3D creates automatically both the tool and the work piece 3D solid models and allows the user to select the motion fragment – step for cutting the work piece (in degrees), as well as the speed (in m/min) and the feed rate (in mm/rev). In addition, a number of parameters for setting up the initial conditions, before the work is initiated, is made available (drill kinematics parameters). Based on the data referred previously, DRILL3D produces two more 3D solid models, one describing the drilling action on the main cutting edge and another for the application of drilling in the area of the chisel edge. These models of the undeformed chip follow a procedure of being segmented into smaller pieces, so that higher accuracy of the thrust force calculation can be achieved. It is worth mentioning that the automatic extraction of the chips' main geometrical characteristics, prior to the calculation of the tool thrust force, integrates the procedure. The complete flow chart of this novel drilling simulation method is presented in Fig. 1.

2.1. Tool description

The DRILL3D routine outputs the Galloway's geometrical description of the tool in a CAD solid model [27]. This solid model of the twist drill fluted part is formed by sweeping helically an appropriate flute cross section for straight cutting lips. The twist drill point geometry is finalized by the Boolean subtraction of the grinding cones, mentioned in Galloway's geometry. According to this model, a range of parameters, separated into two main sets, have to be set in order to produce the desired variety of drilling tools. The first set determines the main shape of the tool (radius, web thickness, half point angle and helix angle), while the second set provides the detail shape of the tool, based on the conventional

grinding method (half cone angle, distance of the cone along the x axis and the y axis).

2.2. Digital drilling process

The digital drilling process is separated into two parts. The first is based on the cutting action of the cutting lips and the second on the cutting action of the chisel edge. Both are treated in a similar way, although individually. The final result is the creation of 3D solid models simulating the undeformed chip and the shape of the remaining work piece geometries for each case. The tool is virtually moved transitionally toward the $-Z$ axis (feed) while at the same time, it is rotated around its Z axis of symmetry using a constant step. In every step, a Boolean subtraction of the tool model, from the remaining work piece model is carried out. The step value, for both cases, is selected comprising the motion accuracy, the calculation complexity and the CAD system capacity. Initially, a specially shaped work piece is used, in order that the cutting lips are directly engaged (steady state case), having a small hole in the middle (chisel edge area). A rotation step of one degree can be successfully incorporated into the model (Fig. 2). Following that, another work piece of pure cylindrical shape with a diameter equal to each tool's chisel edge is used. The step selected in that case, is in the range of three to five degrees in order to achieve the appropriate motion accuracy without encountering software limitations due to the extremely small size of the chip involved. Once more, the undeformed chip produced and the remaining work piece involved, consist the outcome of the virtual cutting process in the area that comes in contact with the chisel edge (Fig. 3). Both cases are very computing intensive and the simulations need to run for a significant amount of cycles in order to achieve constant chip geometry and simulate the steady state condition.

2.3. Force extraction

The 3D models of the undeformed chip, produced earlier from both cases, are segmented into smaller pieces in order to achieve

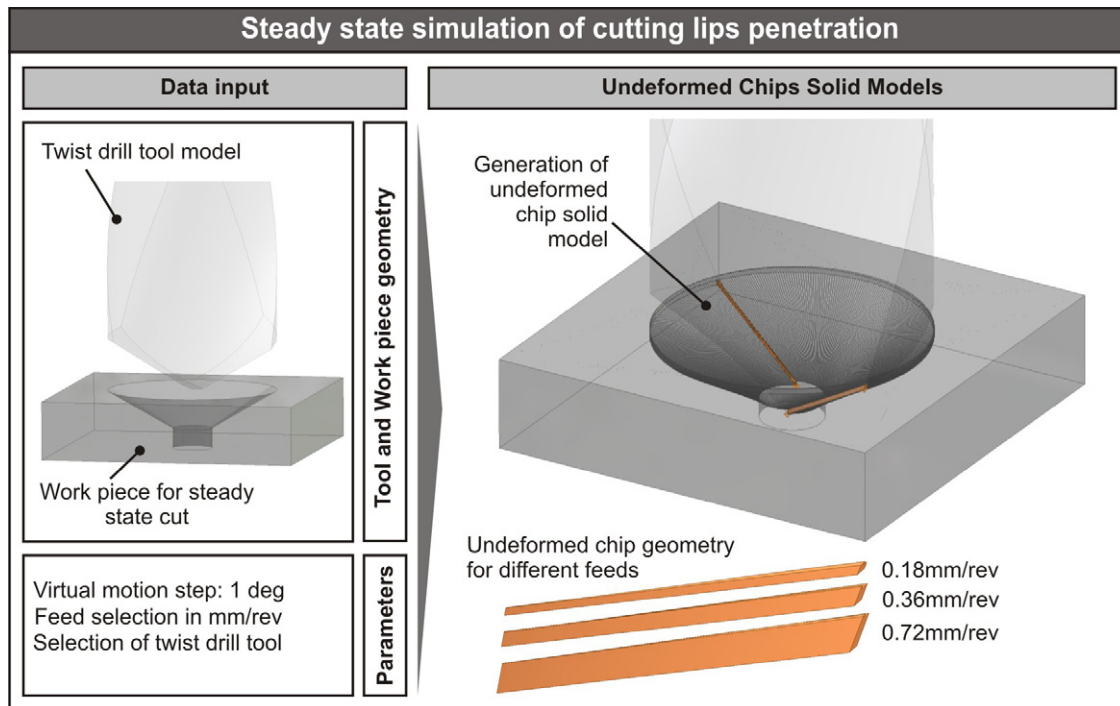


Fig. 2. Steady state simulation of the cutting lips penetration into the remaining work piece.

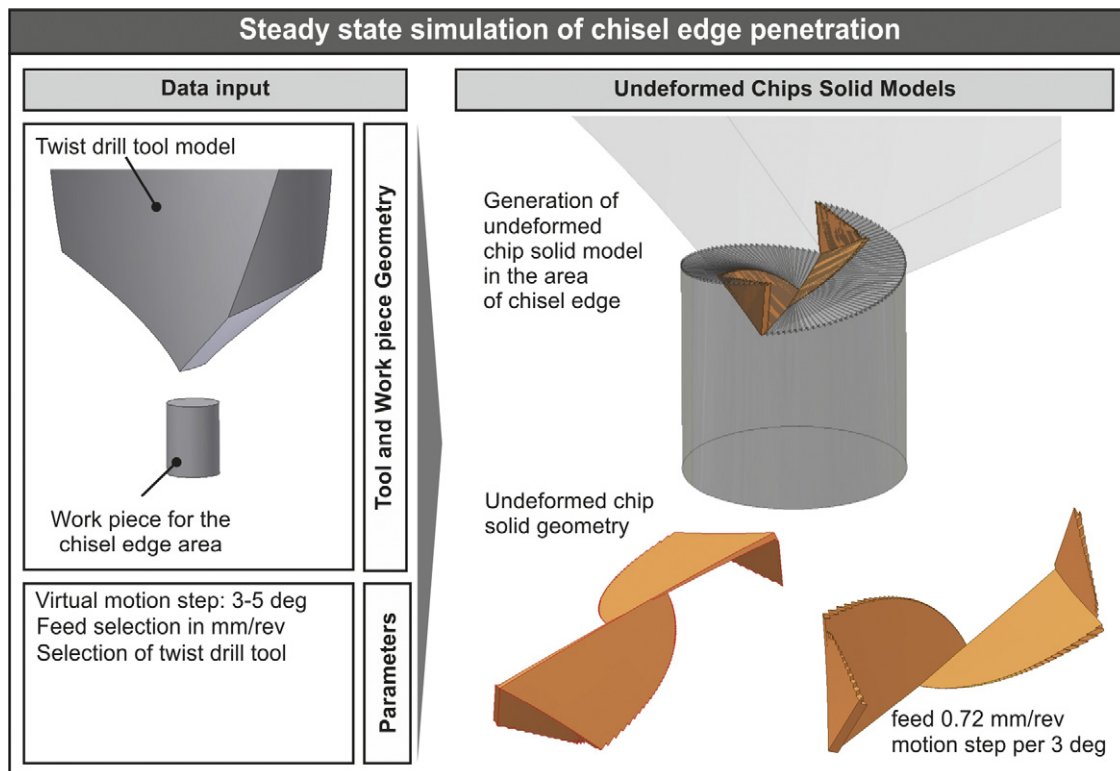


Fig. 3. Steady state simulation of the chisel edge penetration into the remaining work piece.

higher result accuracy. For each individual segmented solid model, a number of geometrical parameters are automatically recognized by the DRILL3D routine, and all this data is introduced as input to the thrust calculation of the tool, based on the Kienzle–Victor method. In more detail, both the undeformed chip width and thickness are directly recognized from each segmented piece of the

solid models, while the selection of the necessary coefficients K_i is made based on published data [28]. Finally, the outcome is the separate calculation of the thrust force for both the tool areas (main cutting edges and chisel edge) by adding up all the primitive force components calculated. An example of a thrust force calculation is analytically presented in Fig. 4.

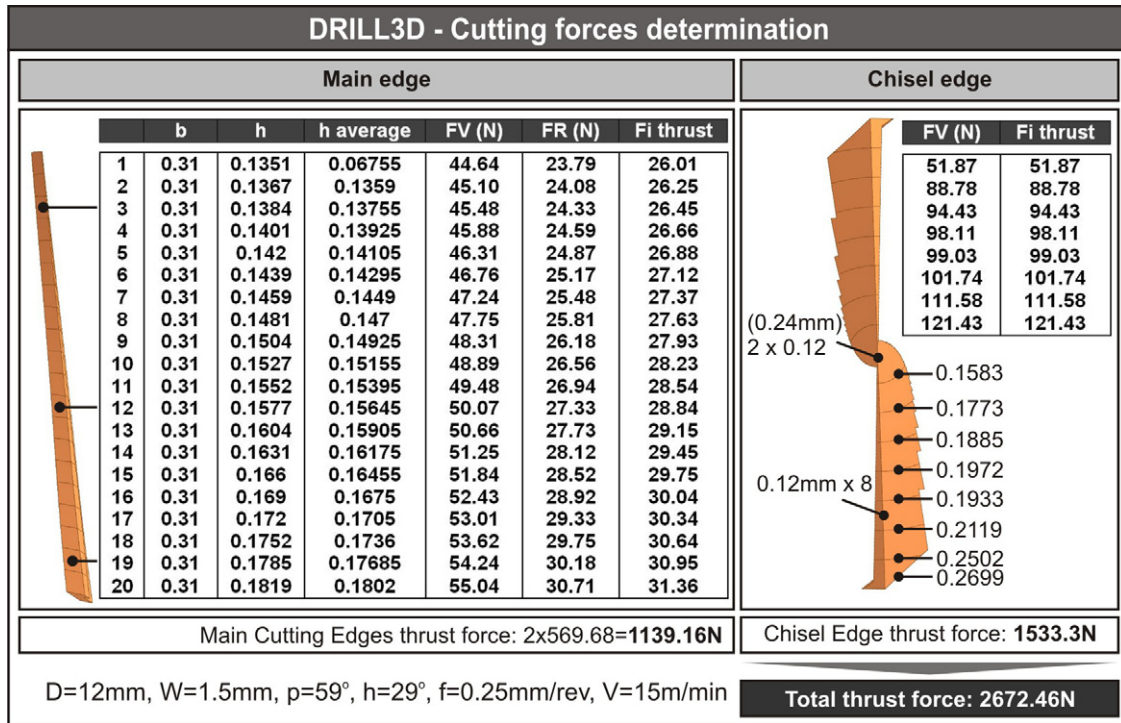


Fig. 4. Example of a thrust force calculation.

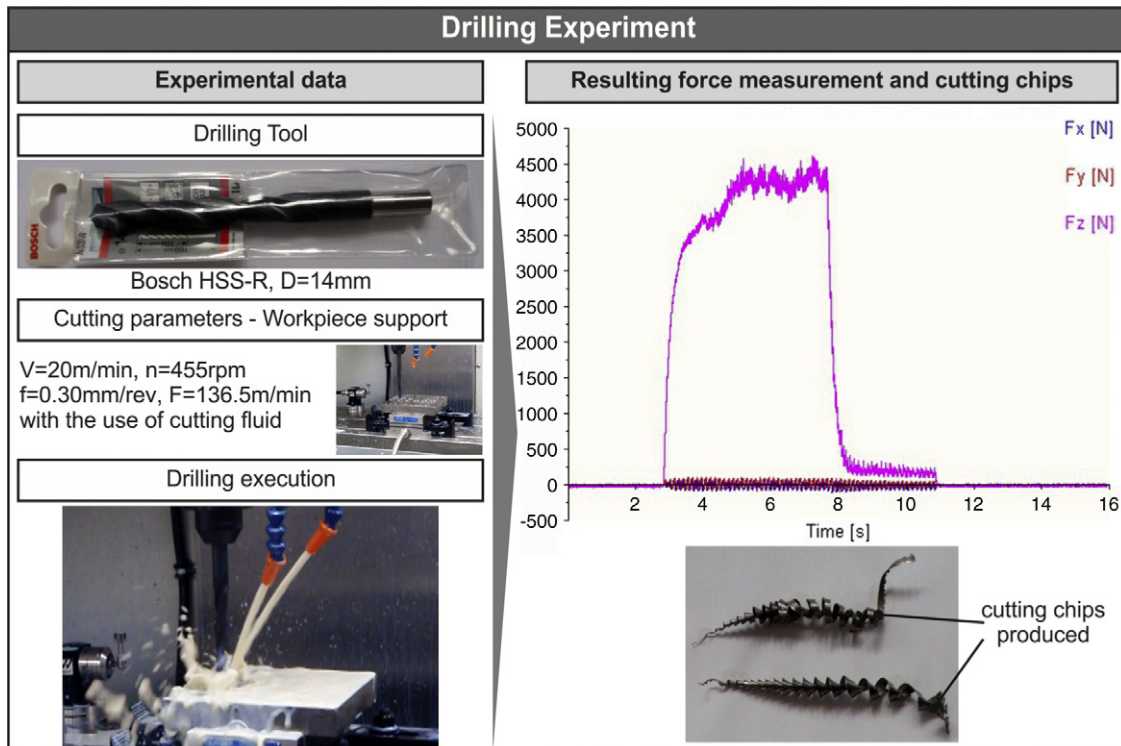


Fig. 5. Drilling experimental results.

2.4. Experimental verification

The accuracy of the DRILL3D drilling simulation model in calculating the thrust force was verified by executing the actual experiments on a HAAS 3-axis CNC machine center with continuous speed and feed control within their boundaries and the specimen

used was a CK60 plate. A Kistler type 9257 BA three component dynamometer was positioned between the machine center and the work piece. The signal was processed by a type 5233 A control unit and during the tests, the thrust force was displayed graphically on the computer monitor and analyzed to enable early error detection and ensure steady state condition (Fig. 5).

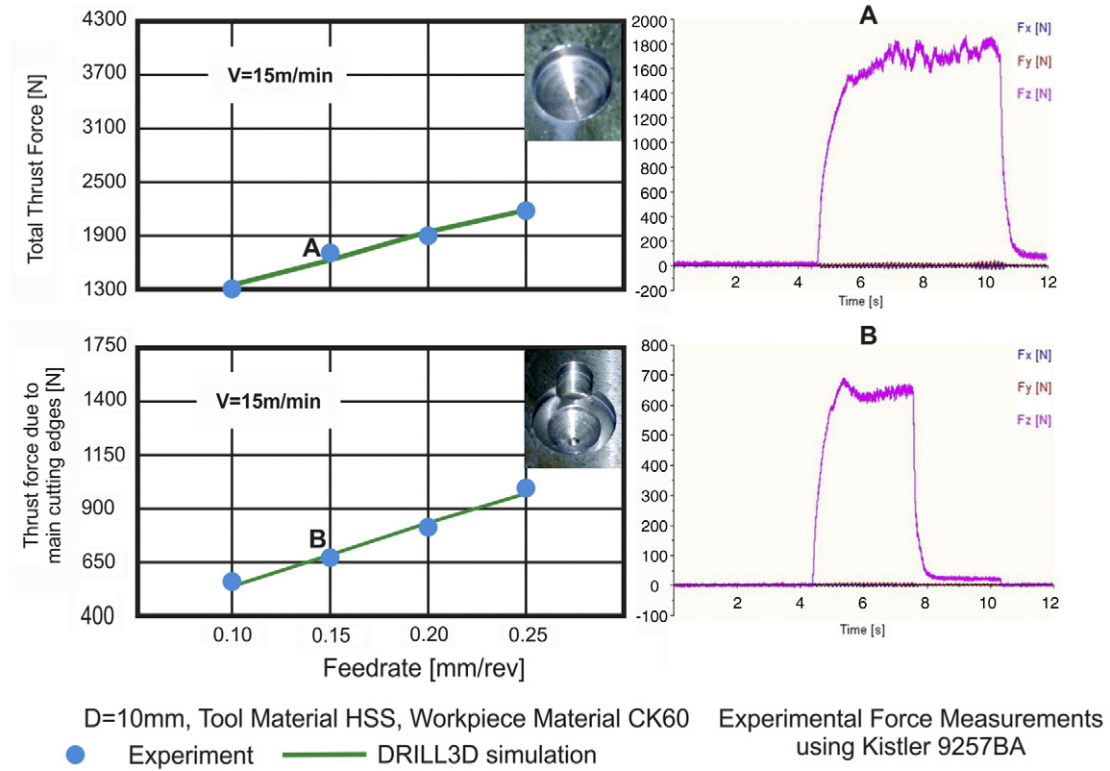


Fig. 6. Thrust force prediction for $D = 10$ mm twist drill tool and $V = 15$ m/min.

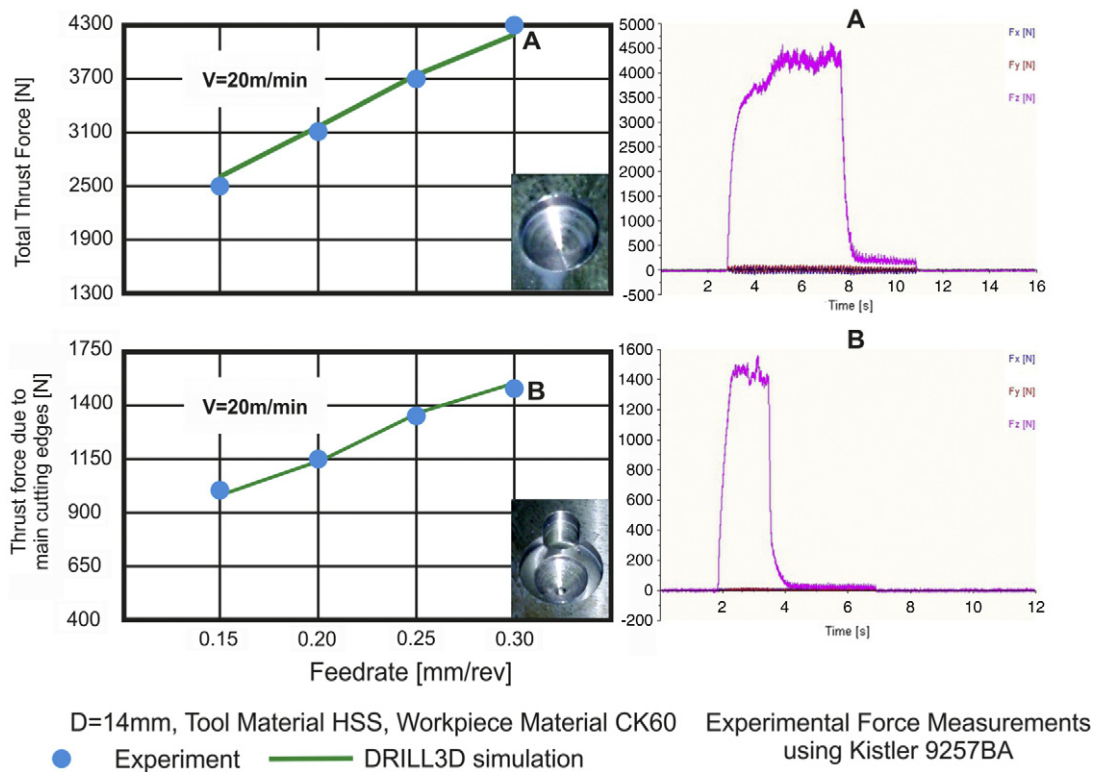


Fig. 7. Thrust force prediction for $D = 14$ mm twist drill tool and $V = 20$ m/min.

In order to be able to separate the thrust force created by the two areas (main cutting edges and chisel edge) two series of experiments were conducted. The first series, involved the direct drill of the work piece, which means that the total thrust force was measured. During the second series, the work piece was preshaped

with a hole in the center. The diameter of the hole was equal to the dimension of the chisel edge and as a result only the thrust force of the main cutting edges was measured. Figs. 6 and 7 depict the thrust force developed in the area of the main cutting lips and the total thrust force applied by the tool during the drilling process. An

Table 1
Factors and levels of drilling parameters.

Factor	Notation	Unit	Levels			
			I	II	III	IV
Tool diameter	<i>D</i>	mm	10	12	14	16
Web to diameter ratio	<i>W/D</i>	–	0.125	0.130	0.145	0.150
Feed rate	<i>f</i>	mm/rev	0.20	0.30	0.40	0.50
Cutting speed	<i>V</i>	m/min	15	20		

indicative number of experimental results are presented together with the results from the DRILL3D simulations so that the accuracy of the proposed approach to be visualized [29].

3. The proposed model for the thrust force using design of experiments

In manufacturing, Design of Experiments (DoE) is found to be an effective statistical technique that can be used for a number of experimental investigations. The technique is one of the powerful tools used in order to investigate the causes of process variation. It is a systematic approach to engineering problem solving, that applies principles at the data collection stage, to ensure the generation of valid defensible and supportable conclusions [30].

The response surface methodology (RSM) is adopted, because a mathematical model can be built easily, with minimal knowledge of the process, requiring less experiments, and thus reducing both cost and time of simulation. The RSM is a statistical modeling tool, which employs the regression analysis to establish the relationship between various process parameters and response. In order to develop the mathematical model, proper planning of the experiments is necessary and the design of experiments technique has been selected for this reason [31,32].

In the present research, the tool diameter (*D*), the web to diameter ratio (*W/D*), the cutting speed (*V*) and the feed rate (*f*) are considered the controllable variables. Table 1 depicts all four factors with their levels, symbols and units used.

For a full factorial analysis, 256 experiments should have been carried out. Half of them are necessary in order to calculate the total thrust force produced by the tool, while the rest are necessary for the determination of the thrust force due to the tool's chisel edge area. The large amount of experiments required, implied the selection of Taguchi's *L*₁₆ table, presented in Table 2, together with the CAD-based experimental results for both the thrust forces. The materials used for all the force calculations were HSS for the drilling tool and CK60 for the working piece.

Table 2
Experimental plan with the computed thrust forces based on Taguchi's *L*₁₆ table.

Exp. no	<i>D</i> (mm)	<i>W/D</i>	<i>f</i> (mm/rev)	<i>V</i> (m/min)	DRILL3D <i>F</i> _{<i>Z</i>_total} (N)	DRILL3D <i>F</i> _{<i>Z</i>_chisel} (N)
1	10	0.125	0.20	15	1916	1072
2	10	0.130	0.30	15	2510	1436
3	10	0.145	0.40	20	3275	2071
4	10	0.150	0.50	20	3864	2511
5	12	0.125	0.30	20	3127	1848
6	12	0.130	0.20	20	2471	1488
7	12	0.145	0.50	15	4337	2747
8	12	0.150	0.40	15	3958	2480
9	14	0.125	0.40	15	4204	2428
10	14	0.130	0.50	15	4876	2918
11	14	0.145	0.20	20	3248	2089
12	14	0.150	0.30	20	4185	2740
13	16	0.125	0.50	20	5933	3615
14	16	0.130	0.40	20	5260	3255
15	16	0.145	0.30	15	4455	2810
16	16	0.150	0.20	15	3520	2257

A polynomial mathematical model was used, so that the total thrust force as well as the thrust force due to the action of the tool's chisel edge area, to be calculated. These models follow the form of

$$\begin{aligned}
 Y = & b_0 + b_1X_1 + b_2X_2 + b_3X_3 + b_4X_4 + b_{11}X_1^2 + b_{22}X_2^2 \\
 & + b_{33}X_3^2 + b_{44}X_4^2 + b_{12}X_1X_2 + b_{13}X_1X_3 + b_{14}X_1X_4 \\
 & + b_{23}X_2X_3 + b_{24}X_2X_4 + b_{34}X_3X_4
 \end{aligned}
 \tag{1}$$

where *Y* is the response i.e. thrust force, *X_i* stands for the coded values for *i* = *D*, *W/D*, *V*, *f*, and *b*₀, . . . , *b*₃₄ represent the regression coefficients.

Using the data illustrated in Table 2 as well as the aforementioned mathematical model, the following equations form the final mathematical model proposed for the calculation of the thrust forces (in N) for both cases (total thrust force and thrust force due to the tool's chisel edge area):

$$\begin{aligned}
 F_{Z_total} = & 9941 - 266.5D - 112015(W/D) - 2045f - 143.24V \\
 & + 5.109D^2 + 343750(W/D)^2 - 5056f^2 \\
 & + 937D(W/D) + 928.4Df + 6.788DV \\
 & + 29603(W/D)f + 715.8(W/D)V
 \end{aligned}
 \tag{2}$$

and

$$\begin{aligned}
 F_{Z_chisel} = & 8124 - 419.9D - 77116(W/D) - 4356f - 104.76V \\
 & + 4.516D^2 + 171250(W/D)^2 - 2318.7f^2 \\
 & - 2062.5D(W/D) + 394.11Df + 5.811DV \\
 & + 37966(W/D)f + 539.6(W/D)V
 \end{aligned}
 \tag{3}$$

where *D* is the tool diameter, (*W/D*) is the web to diameter ratio of the tool, *f* is the feed rate in mm/rev, *V* is the cutting speed used and the tool/work piece materials are HSS/CK60.

(Values highly correlated with other variables have been excluded from the equation.)

4. Analysis of the results and model validation

The adequacy of the models is provided at 95% confidence level. The analysis of variance (ANOVA) has been performed to justify the validity of the model developed. The ANOVA table consists of sum of squares (SS) and degrees of freedom (DF). The sum of squares is usually contributed from the regression model and residual error. Mean square (MS) is the ratio of sum square to the degree of freedom and the *F*-ratio is the ratio of mean square of regression model to the mean square of residual error (Table 3). According to the methodology, the calculated value of *F*-ratio of the developed model, should be more than the tabulated value of *F*-table for 95%

Table 3
ANOVA table for the RSM models.

Source of variation for F_{z_total}	DF	SS	MS	F	P
Regression	12	16 974 569	1 414 547	63 683	0.000
Residual error	3	6 664	2 221		
Total	15	16 981 232			
R-sq (adj)	99.8%				
Source of variation for F_{z_chisel}	DF	SS	MS	F	P
Regression	12	6 927 031	577 253	102 227	0.000
Residual error	3	1 694	565		
Total	15	6 928 725			
R-sq (adj)	99.9%				

F-table (12, 3, 0.05)=8.74

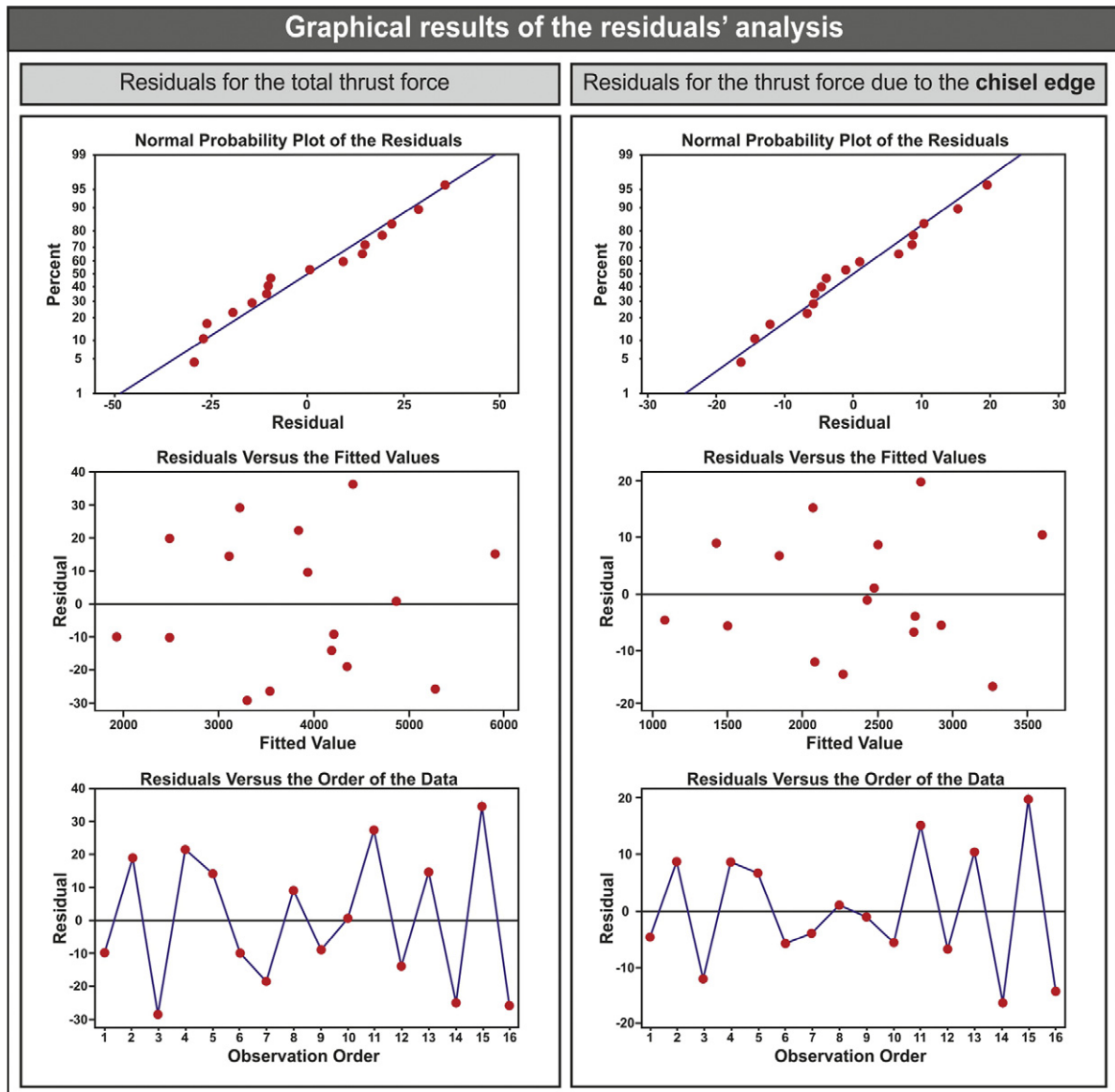


Fig. 8. Residuals analyses for both thrust forces.

confidence level, in order for the model to be adequate (636.83 and 1022.27, respectively, instead of 8.74). In addition, the *P* value is 0.000, which proves the highest correlation, hence the developed response function is quite adequate at a 95% confidence level.

The validity of the fit of the models can also be proved by the adjusted correlation coefficient (*R*-sq (adj)), which provides a measure of variability in observed output and can be explained by

the factors along with the two factor interactions. This coefficient in both cases is well beyond 99% and as a result the models appear to have adequate predictive ability (99.8% and 99.9%, respectively –Table 3).

The accuracy of the models has been checked by the residual analysis, and it is essential that the residuals are normally distributed in order for the regression analysis to be valid. The

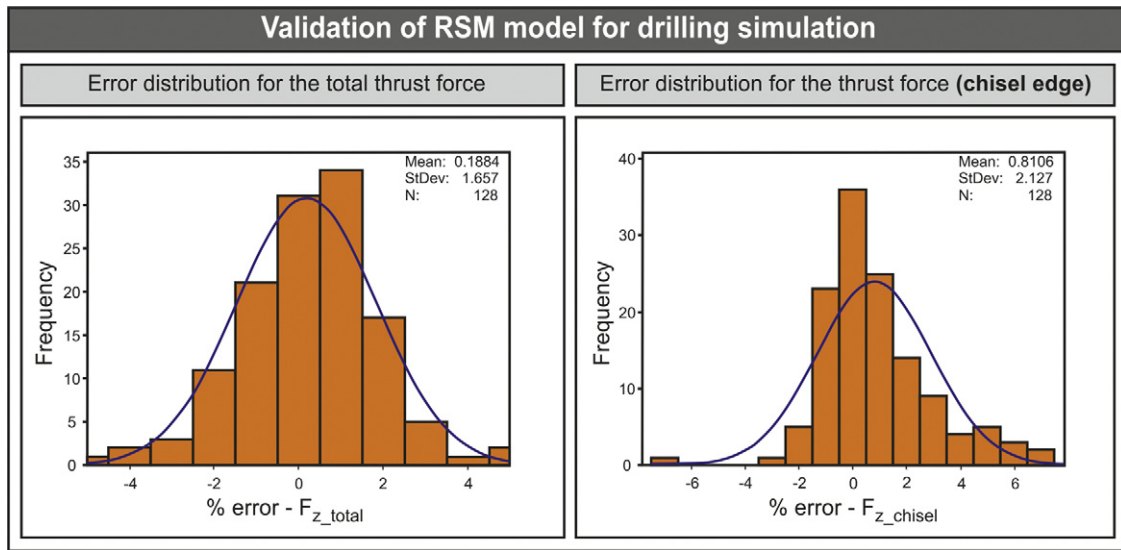


Fig. 9. RSM model validation for the drilling simulation.

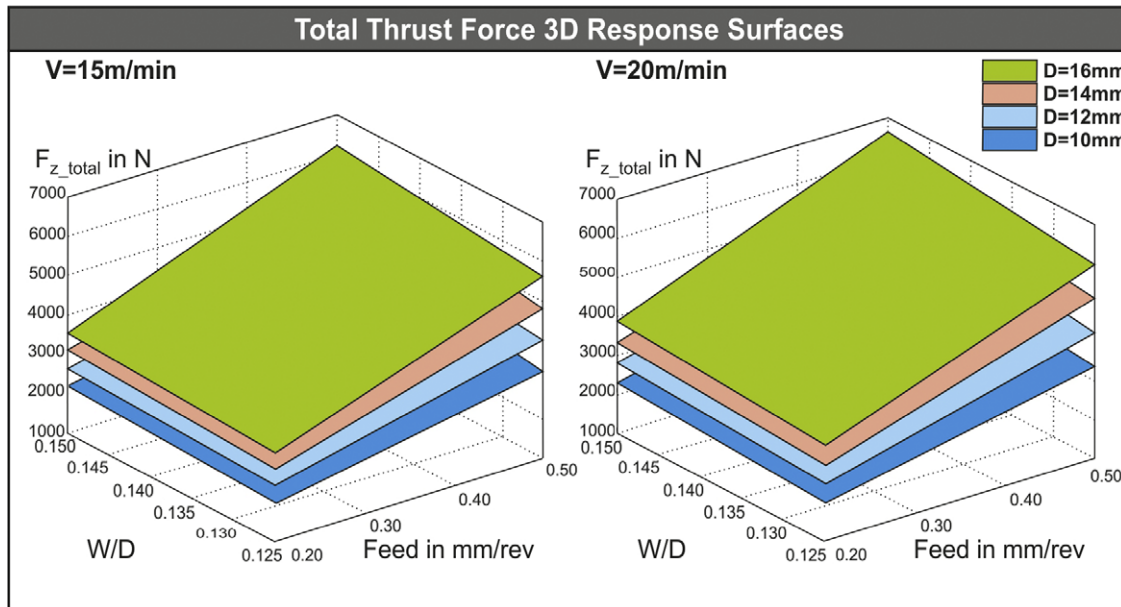


Fig. 10. Total thrust force for four tool diameters.

normal probability plots of the residuals for both the thrust forces calculated are depicted in Fig. 8. The graphs show that the residuals closely follow straight lines (approximately linear pattern), denoting that the errors are normally distributed. In addition, both the scatter diagrams of the thrust force residuals versus the fitted values and the residuals versus the order of the data presented in Fig. 8, depict that the residuals are evenly distributed on both sides of the reference line.

Table 4 depicts the calculation of the thrust forces using the regression models and how these results compare with those calculated by the DRILL3D simulations. All digital experiments were run in order to be able to compare the results for the full factorial set of experiments, in both thrust force cases and validate the mathematical model. Although the regression models were derived from the execution of only 16 experiments, according to the Taguchi L_{16} table, the high accuracy of the predicted thrust forces is proved.

When examining the percentage of difference between the regression and CAD-based models, for all the experiments involved

($N = 128$ in both cases), the higher difference among the results is approx. $\pm 5\%$ for the total thrust force of the tool and approx. $\pm 6.5\%$ for the thrust force due to the chisel edge area (Fig. 9). In addition, in both cases the mean value of the percentage of difference is very close to zero (0.1888% and 0.8106%, respectively) and the resulted standard deviation is limited to 1.657% and 2.127%, respectively. Those limited differences prove the validity of the regression analysis followed and provide a solid basis for the use of a small amount of appropriately selected digital experiments, in order to provide a valid mathematical model for the developed thrust forces in drilling.

The thrust force, in both cases under research, is analyzed through the RSM prediction models by generating 3D response surface plots. Fig. 10 illustrates the total thrust force developed for two different cutting speeds (15 m/min and 20 m/min, respectively) and for four tool diameters each (10 mm, 12 mm, 14 mm and 16 mm). The thrust force increases substantially, when the tool diameter is increased and leads to a smaller but observable rise when the cutting speed becomes higher for a

Table 4
RSM model comparison with DRILL3D for the total thrust force and the thrust force due to the chisel edge.

D (mm)	W/D	f (mm/rev)	V (m/min)	DRILL3D F_{z_total} (N)	RSM F_{z_total} (N)	DRILL3D F_{z_chisel} (N)	RSM F_{z_chisel} (N)	
10	0.125	0.2	15	1916	1925	1072	1076	
			20	2011	1995	1166	1180	
		0.3	15	2458	2466	1380	1394	
			20	2579	2536	1501	1498	
		0.4	15	2822	2906	1640	1664	
			20	2966	2976	1784	1768	
	0.13	0.5	15	3289	3245	1901	1889	
			20	3456	3315	2067	1993	
		0.2	15	1927	1933	1098	1091	
			20	2023	2022	1194	1208	
		0.3	15	2510	2489	1436	1427	
			20	2636	2577	1562	1544	
	0.145	0.4	15	2903	2944	1726	1717	
			20	3055	3032	1878	1834	
		0.5	15	3394	3298	2012	1960	
			20	3570	3386	2189	2078	
		0.2	15	2089	2061	1271	1185	
			20	2200	2203	1382	1343	
	0.15	0.3	15	2673	2662	1614	1578	
			20	2815	2804	1755	1736	
		0.4	15	3108	3161	1904	1925	
			20	3275	3303	2071	2083	
		0.5	15	3586	3559	2225	2225	
			20	3782	3701	2421	2383	
	12	0.125	0.2	15	2088	2138	1274	1234
				20	2200	2298	1385	1405
			0.3	15	2722	2753	1667	1646
				20	2868	2914	1813	1817
			0.4	15	3146	3267	1993	2011
				20	3321	3428	2168	2183
0.13		0.5	15	3662	3680	2309	2331	
			20	3864	3840	2511	2502	
		0.2	15	2284	2306	1297	1283	
			20	2398	2444	1410	1445	
		0.3	15	2978	2973	1699	1679	
			20	3127	3111	1848	1841	
0.145		0.4	15	3544	3538	2030	2029	
			20	3722	3677	2208	2191	
		0.5	15	3963	4003	2337	2332	
			20	4168	4141	2542	2494	
		0.2	15	2351	2323	1368	1318	
			20	2471	2480	1488	1493	
0.15		0.3	15	3057	3005	1783	1733	
			20	3213	3161	1939	1908	
		0.4	15	3650	3586	2143	2101	
			20	3838	3742	2331	2277	
		0.5	15	4076	4065	2459	2424	
			20	4291	4221	2675	2599	
12		0.125	0.2	15	2553	2480	1584	1474
				20	2692	2690	1722	1690
			0.3	15	3271	3206	2015	1946
				20	3448	3416	2192	2162
			0.4	15	3862	3831	2376	2372
				20	4071	4041	2585	2588
	0.13	0.5	15	4337	4354	2747	2751	
			20	4578	4565	2988	2967	
		0.2	15	2588	2566	1624	1543	
			20	2731	2794	1766	1773	
		0.3	15	3349	3307	2099	2034	
			20	3533	3535	2283	2264	
	0.145	0.4	15	3958	3947	2480	2479	
			20	4175	4175	2697	2708	
		0.5	15	4417	4485	2842	2877	
			20	4666	4713	3091	3106	

(continued on next page)

Table 4 (continued)

D (mm)	W/D	f (mm/rev)	V (m/min)	DRILL3D F_{z_total} (N)	RSM F_{z_total} (N)	DRILL3D F_{z_chisel} (N)	RSM F_{z_chisel} (N)
14	0.125	0.2	15	2727	2728	1586	1526
			20	2866	2934	1725	1746
		0.3	15	3527	3520	2047	2000
			20	3706	3727	2226	2221
		0.4	15	4204	4212	2428	2429
			20	4417	4418	2641	2649
	0.5	15	4742	4802	2775	2811	
		20	4985	5008	3018	3031	
	0.13	0.2	15	2806	2755	1670	1581
			20	2953	2979	1817	1815
		0.3	15	3631	3562	2159	2075
			20	3821	3786	2348	2309
		0.4	15	4301	4268	2534	2522
			20	4523	4492	2756	2756
	0.5	15	4876	4873	2918	2923	
		20	5132	5098	3174	3157	
	0.145	0.2	15	3079	2939	1921	1799
			20	3248	3217	2089	2073
		0.3	15	3886	3791	2435	2350
			20	4099	4069	2648	2624
		0.4	15	4634	4541	2893	2854
			20	4888	4819	3147	3128
	0.5	15	5292	5191	3363	3312	
		20	5587	5469	3658	3586	
0.15	0.2	15	3131	3035	2016	1889	
		20	3307	3331	2193	2177	
	0.3	15	3964	3901	2519	2459	
		20	4185	4197	2740	2746	
	0.4	15	4595	4667	2918	2982	
		20	4851	4963	3174	3270	
0.5	15	5256	5331	3420	3459		
	20	5556	5627	3720	3747		
0.125	0.2	15	3192	3190	1896	1804	
		20	3358	3465	2063	2083	
	0.3	15	4084	4109	2405	2358	
		20	4295	4383	2616	2636	
	0.4	15	4872	4926	2857	2865	
		20	5123	5200	3108	3144	
0.5	15	5641	5642	3323	3326		
	20	5933	5916	3615	3604		
0.13	0.2	15	3296	3227	2006	1881	
		20	3472	3519	2182	2172	
	0.3	15	4196	4160	2525	2453	
		20	4417	4452	2747	2745	
	0.4	15	4997	4992	2993	2979	
		20	5260	5284	3255	3271	
0.5	15	5754	5723	3448	3459		
	20	6056	6015	3750	3751		
0.145	0.2	15	3543	3439	2274	2160	
		20	3743	3785	2474	2493	
	0.3	15	4455	4417	2810	2790	
		20	4701	4763	3057	3122	
	0.4	15	5366	5293	3392	3373	
		20	5663	5639	3690	3706	
0.5	15	6114	6068	3843	3910		
	20	6451	6414	4181	4242		
0.15	0.2	15	3520	3545	2257	2271	
		20	3718	3908	2455	2617	
	0.3	15	4587	4537	2951	2919	
		20	4846	4901	3210	3265	
	0.4	15	5523	5428	3560	3522	
		20	5835	5792	3872	3867	
0.5	15	6283	6218	4024	4077		
	20	6636	6582	4377	4423		

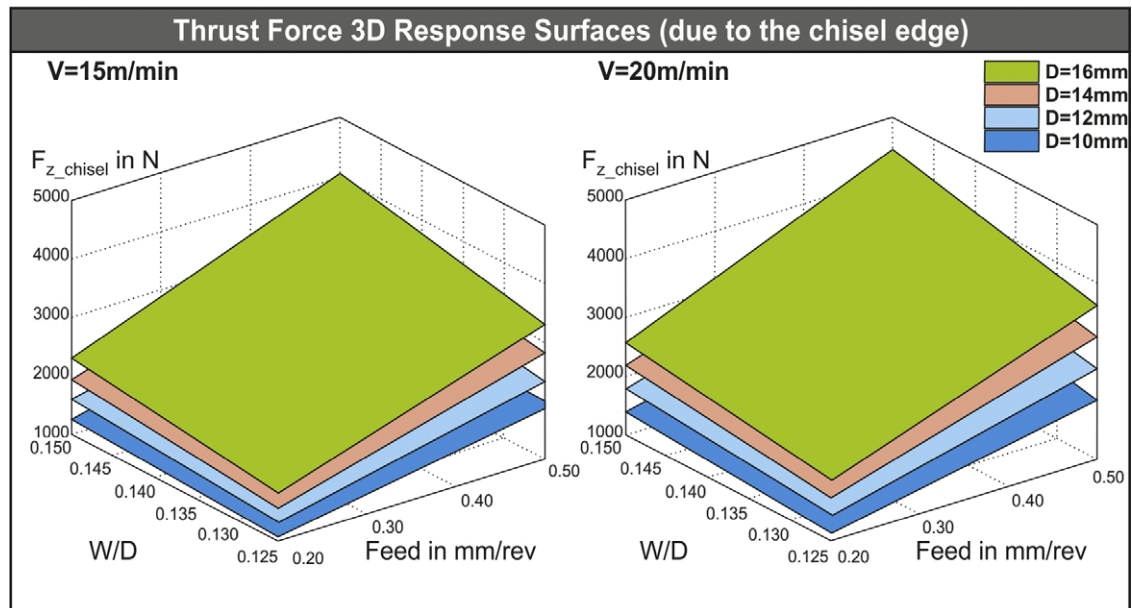


Fig. 11. Thrust force due to the chisel edge for four tool diameters.

constant diameter. A similar trend of the thrust force due to the chisel edge area is illustrated in Fig. 11.

5. Conclusions

A combined use of CAD-based simulation and design of experiments has been presented in this paper, in order to accurately calculate the developed thrust force on a drilling tool. The thrust forces under consideration involved both the total thrust force and the thrust force due to the action of the chisel edge area. They were both studied with respect to the tool diameter, the web to diameter ratio, the feed rate and the cutting speed used. The full factorial analysis would demand 256 experiments; so design of experiments was adopted in order to reduce the amount of the experiments. All the experimental work was based on DRILL3D, a novel drilling simulation application, which has been validated in the previously published research work.

The combination of the CAD-based drilling simulation and the design of experiments methodology was used in order to achieve higher level of verification, while at the same time to radically reduce the cost of the necessary experimental effort. The mathematical models produced based on the RSM methodology, proved to be very accurate and extremely easy to use since they provide a function, which can be used directly in a variety of other applications.

References

- [1] Grzesik W. Advanced machining processes of metallic materials. Elsevier; 2008.
- [2] Armarego EJA. The unified-generalized mechanics of cutting approach—a step towards a house of predictive performance models for machining operations. *Machining Science & Technology* 2000;4(3):319–62.
- [3] Kang D, Armarego EJA. Computer-aided geometrical analysis of the fluting operation for the twist drill design and production. I. Forward analysis and generated flute profile. *Machining Science & Technology* 2003;7(2):221–48.
- [4] Kang D, Armarego EJA. Computer-aided geometrical analysis of the fluting operation for the twist drill design and production. II. Backward analysis, wheel profile and simulation studies. *Machining Science & Technology* 2003;7(2):249–66.
- [5] Wang J, Zhang QA. A study of high-performance plane rake faced twist drills. Part II: predictive force models. *International Journal of Machine Tools and Manufacture* 2008;48:1286–95.
- [6] Paul A, Kappor SG, Devor RE. Chisel edge and cutting lip shape optimization for improved twist drill point design. *International Journal of Machine Tools and Manufacture* 2005;45:421–31.
- [7] Koehler W. Analysis of the high performance drilling process: influence of shape and profile of cutting edge of twist drills. *Journal of Manufacturing Science and Engineering* 2008; doi:10.1115/1.2951932.
- [8] Claudin C, Poulachon G, Lambertin M. Correlation between drill geometry and mechanical forces in MQL conditions. *Machining Science & Technology* 2008;12:133–44.
- [9] Abrao AM, Rubio JCC, Faria PE, Davim JP. The effect of cutting tool geometry on thrust force and delamination when drilling glass fibre reinforced plastic composite. *Materials and Design* 2008;29:508–13.
- [10] Hamade RF, Seif CY, Ismail F. Extracting cutting force coefficients from drilling experiments. *International Journal of Machine Tools & Manufacture* 2006;46:387–96.
- [11] Singh I, Bhatnagar N, Viswanath P. Drilling of uni-directional glass fiber reinforcement plastics: experimental and finite element study. *Materials and Design* 2008;29:546–53.
- [12] Strenkowski JS, Hsieh CC, Shih AJ. An analytical finite element technique for predicting thrust force and torque in drilling. *International Journal of Machine Tools and Manufacture* 2004;44:1413–21.
- [13] Zitoune R, Collombet F. Numerical prediction of the thrust force responsible of delamination during the drilling of the long fibre composite structures. *Composites Part A: Applied Science and Manufacturing* 2007;38:858–66.
- [14] Kadrigama K, Abou-El-Hossein KA, Mohammad B, Habeeb AA, Noor MM. Cutting force prediction model by FEA and RSM when machining Hastelloy C-22HS with 90° holder. *Journal of Scientific & Industrial Research* 2008;67:421–7.
- [15] Bagci E, Ozelcik B. Finite element and experimental investigation of temperature changes on a twist drill in sequential dry drilling. *International Journal of Advanced Manufacturing Technology* 2006;28:680–7.
- [16] Vijayaraghavan A, Dornfeld D. Automated drill modeling for drilling process simulation. *Journal of Computing and Information Science in Engineering* 2007;7:276–83.
- [17] Chandrasekaran M, Muralidhar M, Murali KC, Dixit US. Application of computing techniques in machining performance prediction and optimization: a literature review. *International Journal of Advanced Manufacturing Technology* 2010;46:445–64.
- [18] Laporte S, K'Nevez JY, Cahuc O. Phenomenological model for drilling operation. *International Journal of Advanced Manufacturing Technology* 2009;40:1–11.
- [19] Tsao CC. Taguchi analysis of drilling quality associated with core drill in drilling of composite material. *International Journal of Advanced Manufacturing Technology* 2007;32:877–84.
- [20] Tsao CC. Prediction of thrust force of step drill in drilling composite material by Taguchi method and radial basis function network. *International Journal of Advanced Manufacturing Technology* 2008;36:11–8.
- [21] Tsao CC, Hocheng H. Evaluation of thrust force and surface roughness in drilling composite material using Taguchi analysis and neural network. *Journal of Materials Processing Technology* 2008;203:342–8.
- [22] Basavarajappa S, Chandramohan G, Davim JP. Some studies on drilling of hybrid metal matrix composites based on Taguchi techniques. *Journal of Materials Processing Technology* 2008;196:332–8.
- [23] Hayajneh MT, Hassan AM, Mayyas AT. Artificial neural network modeling of the drilling process of self-lubricated aluminium/alumina/graphite hybrid composites synthesized by powder metallurgy technique. *Journal of Alloys and Compounds* 2009;478:559–65.

- [24] Zhang JZ, Chen JC. Surface roughness optimisation in a drilling operation using the Taguchi design method. *Materials and Manufacturing Processes* 2009;24: 459–67.
- [25] Kyratsis P, Bilalis N, Antoniadis A. CAD based predictive models of the undeformed chip geometry in drilling. *International Journal of Mechanical Systems Science and Engineering* 2009;1:129–35.
- [26] Kyratsis P, Tapoglou N, Bilalis N, Antoniadis A. Thrust force prediction of twist drill tools using a 3D CAD system application programming interface. *International Journal of Machining and Machinability of Materials* [in press].
- [27] Galloway G. Some experiments on the influence of various factors on drill performance. *ASME Transactions* 1957;79:191–231.
- [28] König W, Essel K. Spezifische schnittkraftwerte für die zerspannung metallischer werkstoffe. Dusseldorf: Verlag Stahleisen MBH; 1973.
- [29] Kyratsis P. Simulation of the drilling manufacturing process using a CAD/CAM system. Ph.D. thesis. Technical University of Crete; 2011.
- [30] Cochran WG, Cox GM. *Experimental design*. New York: John Wiley and Sons; 1992.
- [31] Montgomery DC. *Design and analysis of experiments*. New York: John Wiley and Sons; 2001.
- [32] Myers RH, Montgomery DC. *Response surface methodology: process and product optimization using designed experiments*. New York: John Wiley and Sons; 1995.